Growth and characterization of Glycinium Cyanoacetate (GCA) single crystals

R. Subash Chandra Bose[1], K.Balasubramanian[2], R.Subramaniyan@Raja[3], K.Anuradha[4]

1 Research Scholar (Reg. No.17211072131024)

1, 2 PG & Research Department of Physics, The M.D.T. Hindu College, Tirunelveli 627010, Tamilnadu, India

(Affiliated to Manonmaniam Sundaranar University, Abishekapatti, Tirunelveli 627012, Tamilnadu, India)

3 Department of Physics, KPR Institute of Engineering and Technology, Coimbatore-641407, Tamilnadu, India.

4 Department of Physics, Methodist College of Engineering and Technology, Abids, Hyderabad, Telangana, 500001, India

Corresponding author mail id : subashchandrabose@mdthinducollege.org

Abstract:

Glycine and cyanoacetic acid were combined in a 1:1 ratio to grow Glycinium Cyanoacetate (GCA) crystals, which were then slowly grown as single crystals in methanol as a solvent. Unit cell attributes were discovered via single-crystal X-ray diffraction. Functional groups were found in GCA using FTIR spectra. The linear optical properties of solution-grown GCA crystals were studied in UV-Vis spectrometers. Vickers Microhardness Tester was used to assess the mechanical properties of the crystal. TG/DTA study was carried out to find the thermal stability and water of crystallization. The transmittance and absorbance behaviour of the sample has been tested by UV-visible spectral studies The LDT value of GCA crystal was found by using Nd: YAG laser The antibacterial properties of the GCA were evaluated using the Agar disc diffusion method.

Introduction

Organic non-linear optical crystals are very important because they have great qualities in many fields, such as photonics, optical switching, optoelectronics, optical communication systems, and laser technology [1]. The existence of the d-A conjugate system, which increases the asymmetric polarizability of the organic crystals, gives them the potential for strong nonlinear optical properties [2]. Due to their significant electrical conductivity, organic molecules with inter and intramolecular charge transfer interactions are now crucial in the creation of photovoltaic and different optoelectronic devices [3]. A strong organic base with an excellent hydrogen bond acceptor is produced by pyridine, and this base is employed to make optical nonlinear materials and photochemicals [4]. Special physical and chemical characteristics make them ideal for use as catalysts and reagents in organic materials, light-emitting diodes (LED), powerful fluorescent dyes, and nonlinear optical applications [5]. Glycine (C2H5O2N) is the amino acid with the lowest molecular weight. Glycine is an amino acid that is white and see-through. It is found in many proteins. It has something to do with sour acid. It's also known as amino acetic acid. It is the easiest of the twenty common amino acids, and it makes up about 33% of the structures of collagen. It has been used a lot in

creating crystals. Unlike other amino acids, it does not have an asymmetric carbon and is visually inactive. It doesn't have both D and L stereoisomers. It is the main amino acid that changes the shape of proteins and has no centre of chirality. It exists in the arrangement as zwitterions and in a strong state. Even though there are different reports on this compound, the amazing qualities of crystals in the glycine family drive the research to look into it more. But nonlinear optical second harmonic generation [6-8] is expected to happen only in glycine complexes that crystallise in a structure that is not centred around a point. Most of the parts of amino acids are nonlinear optical (NLO) materials that can be used in different ways for optical communication, optical figuring, optical data processing, and photonics. The cyanoacetic acid nitrile group, which acts as an acid source, improves the flame-retarding effect [9-10]. Polyester electro optic materials and the polymerization procedure both use carbonyl groups [11-12]. In conjugated molecules, both the electron donor and acceptor display exceptionally high optical nonlinearity. With the use of theoretical and experimental research, the current study aims to comprehend the spectroscopic characteristics of GCA To compare the structural activity study and non-linear optical activity with GCA, the compared chemicals, such as Glycine (G) and cyanoacetic acid (CY), have been chosen.

Material Synthesis

Crystals made of analytical-grade synthetic chemicals from the glycine and 2- cyanoacetic acid are taken 1:1 ratio were mixed with double-deionized water using a magnetic stirrer to get a uniform focus at the room temperature and the reaction scheme is depicted in Fig 1.

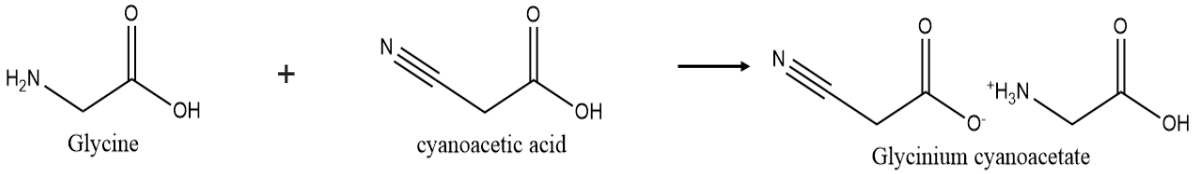

Fig 1. Reaction scheme of GCA crystals

The supersaturated solution was filtered through Whatman filter paper and left to slowly evaporate at room temperature over a month. This process, called the cycle of nucleation and grain development, led to crystals with good visual quality. The high-quality single crystals were harvested over a forty-day period via continuous evaporation. Fig. 2 is the photograph of as grown crystals of GCA . Physical and chemical tests were done on the single crystals of good quality.

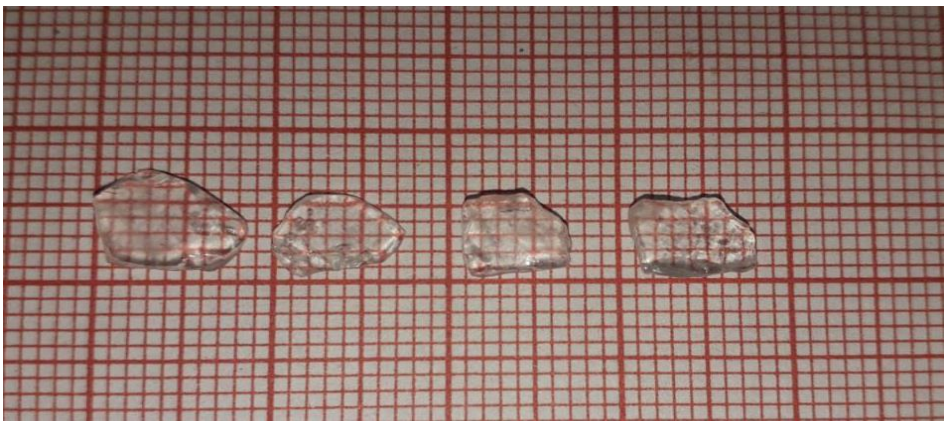

Fig 2. Photograph of GCA crystals

Characterization Studies

The combination was tested with X-ray diffraction using a Bruker Kappa Apex II diffractometer and monochromated MoKα radiation (= 0.71073Å). Data collection, data reduction and absorption corrections were performed by APEX2, SAINTplus and SADABS programs [14]. The structure was solved by direct methods procedure using SHELXS-2016 program and refined by Full-matrix least squares procedure on F^2 [14] reflections in three different crystallographic zones were used to figure out the characteristics of the unit cell. The purity and crystallinity of GCA crystals have been confirmed by recording powder X-ray diffraction pattern using a REICH SEIFERT X-ray diffractometer employing Cu Ka (1.54058 Å) with a scan speed of 1°/min over a range of 10–80°. We used a SHIMADZU SPECTROMETER UV-1800 to measure the linear optical properties of GCA single crystals from 200 nm to 1100 nm. TGA and DTA were used to figure out how the GCA sample reacted to heat. The TG/DTA was done in a nitrogen atmosphere at a rate of 100°C per minute over a temperature range of 30 to 500°C. To explore the laser damaged threshold, a Q-switched high intensity Nd-YAG laser source with a wavelength of 1064 nm and a plus width of 6 ns, repeated at 10 Hz, was employed. The power of the laser was concentrated at a 15 cm converging lens's near focus. To get the most power out, increase the power density of the fundamental beam, which is related to the efficiency of the harmonic conversion.

Results and discussion

The crystal possess Triclinic structure with space group P-1. Lattice parameter values determined are as follows: a = 5.4497(3) Å , b = b = 8.0074(4) Å, c = 9.2928(5) Å , α=70.081 (2) β = 74.017(2)°. γ = 81.934(2)° and cell volume = 366.04(3)$Å^3$. The molecular structure of GCA crystal is shown in Fig 3. Table.1 summarizes the crystallographic data and structure refinement for grown GCA. The structure was solved by direct methods, are refined to

R = 0.0586 for 2082 independent reflections. A three-dimensional network of hydrogen bonds stabilizes the crystal structure. Table 2 gives the details of Atomic coordinates (x 10^4) and equivalent isotropic displacement parameters ($Å^2$x 10^3) for GCA. U(eq) is defined as one third of the trace of the orthogonalized U^{ij} tensor. The cyanoacetate group is involved H bonds N(1)-H(1A) 0.960(16) and O(2)-H(2) 1.2142(8) Å, respectively. The bond lengths and bond angles are given in Table 3. Strong N-H-O, intermolecular, and intramolecular hydrogen bonds help to stabilise the crystalline salt. Most cyanoacetate salts exhibit the O-H-O intramolecular hydrogen bond, which creates a S (6) ring motif, as a common property. For intensities I > 2 (I), the final least-squares refinement converges to an R1 = 0.0370, wR2 = 0.1006. Fig. 2 displays the GCA molecular structure. Using the ORTEP3 programme, the thermal ellipsoid of the GCA drawing was created [15] and shown in Fig 4. The anionic-cationic-solvent molecule formed by the anionic-cationic-solvent bond between the glycinium cation and the molecular sheet which generates the crystalline solid and shown in Fig 5. Table 4. Hydrogen coordinates (x 104) and isotropic displacement parameters.

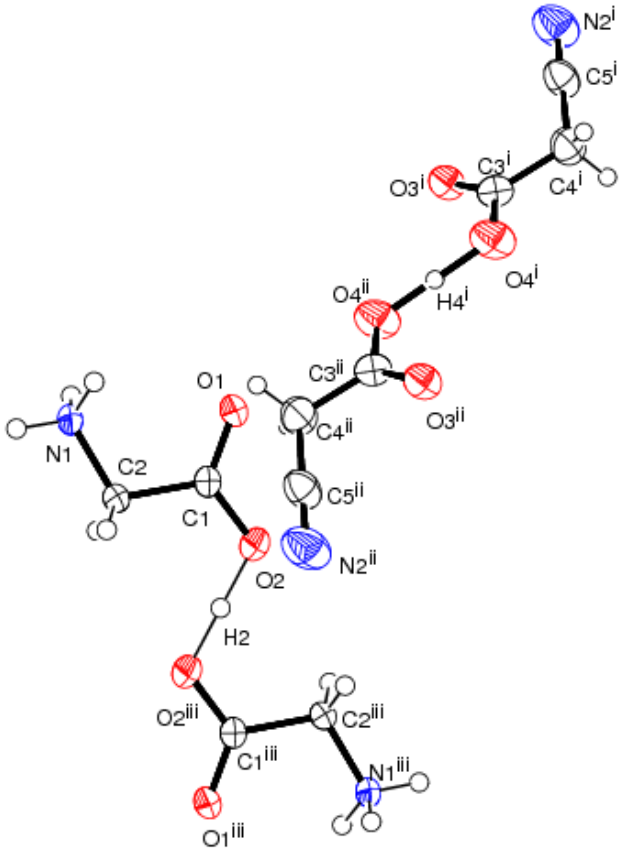

Fig 3. Molecular Structure of GCA

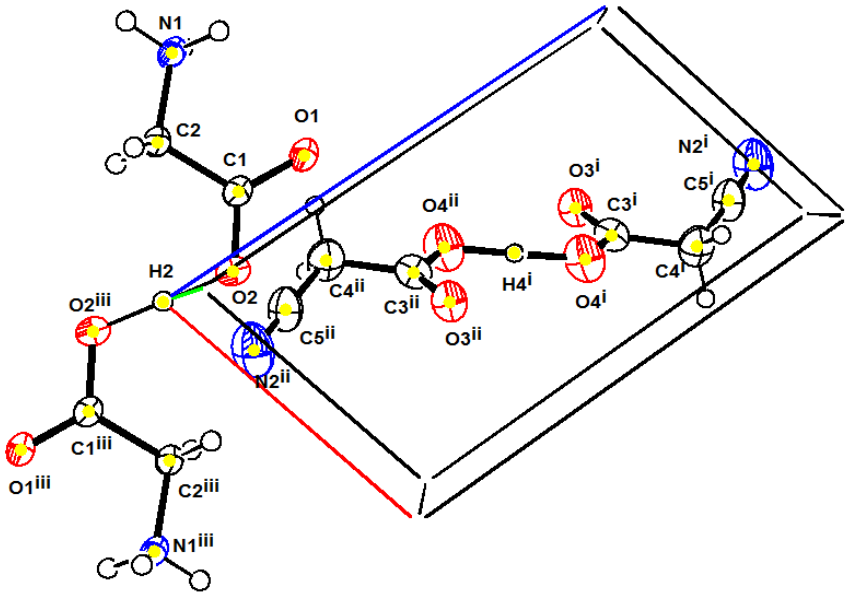

Fig 4.Ortep diagram of GCA

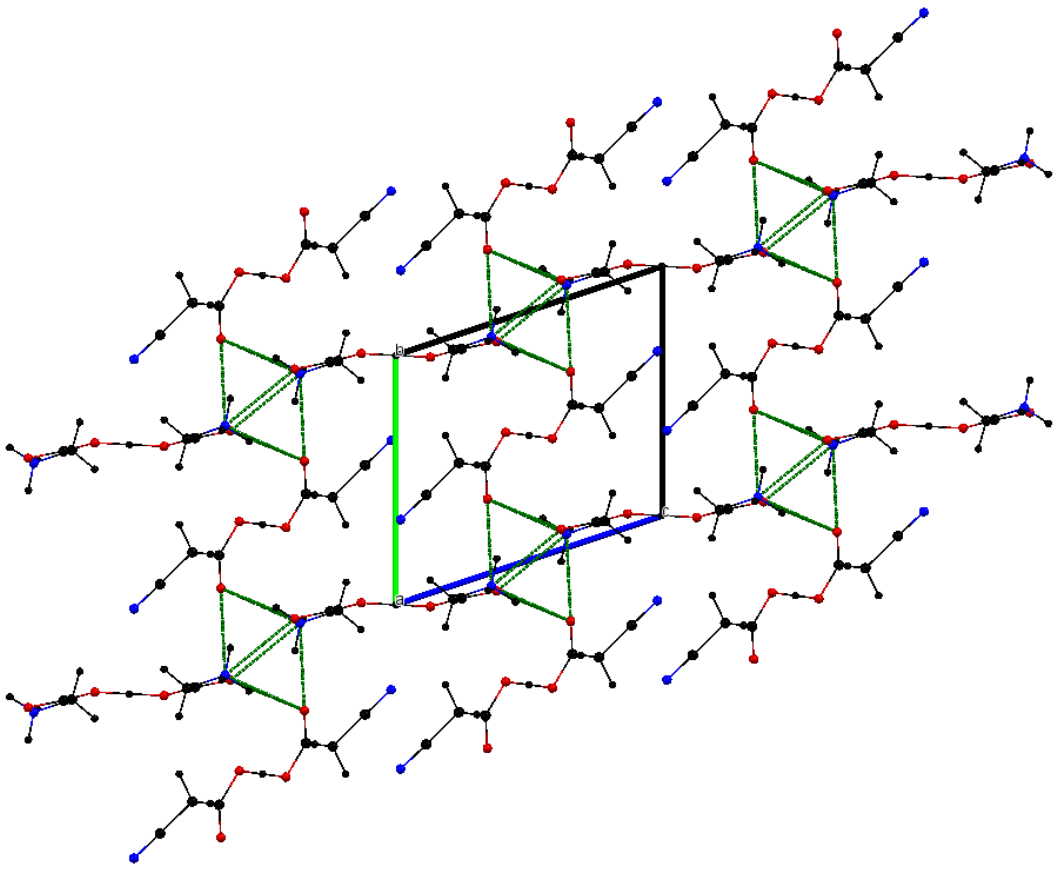

Fig 5. Molecular Sheet of GCA

Table 1. Crystal data and structure refinement for GCA

Identification code	GCA
Empirical formula	C10 H16 N4 O8
Formula weight	320.27
Temperature	296(2) K
Wavelength	0.71073 Å
Crystal system	Triclinic
Space group	P -1
Unit cell dimensions	a = 5.4497(3) Å, α= 70.081(2)°.
	b = 8.0074(4) Å, β= 74.017(2)°.
	c = 9.2928(5) Å, γ= 81.934(2)°.
Volume	366.04(3) $Å^3$
Z	1
Density (calculated)	1.453 Mg/m^3
Absorption coefficient	0.127 mm^{-1}
F(000)	168
Crystal size	0.180 x 0.150 x 0.120 mm3
Theta range for data collection	2.404 to 29.751°.

Index ranges	-7<=h<=7, -11<=k<=11, -12<=l<=12
Reflections collected	11589
Independent reflections	2082 [R(int) = 0.0586]
Completeness to theta = 25.242°	100.00%
Absorption correction	Semi-empirical from equivalents
Max. and min. transmission	0.7458 and 0.6357
Refinement method	Full-matrix least-squares on F^2
Data / restraints / parameters	2082 / 0 / 115
Goodness-of-fit on F2	1.066
Final R indices [I>2sigma(I)]	R1 = 0.0370, wR2 = 0.1006
R indices (all data)	R1 = 0.0449, wR2 = 0.1068
Extinction coefficient	0.26(2)
Largest diff. peak and hole	0.348 and -0.209 e.$Å^{-3}$

Table 2. Atomic coordinates (x 10^4) and equivalent isotropic displacement parameters ($Å^2$x 10^3) for GCA. U(eq) is defined as one third of the trace of the orthogonalized U^{ij} tensor.

	x	y	z	U(eq)
C(1)	8506(2)	9381(1)	2467(1)	26(1)
C(2)	5895(2)	9454(1)	2166(1)	27(1)
C(3)	6390(2)	5650(1)	6632(1)	35(1)
C(4)	8328(3)	5159(2)	7631(2)	47(1)
C(5)	7734(3)	6012(2)	8852(2)	44(1)
N(1)	3884(2)	9459(1)	3592(1)	27(1)
N(2)	7236(3)	6652(2)	9821(2)	64(1)
O(1)	8702(1)	9193(1)	3795(1)	42(1)
O(2)	10440(1)	9463(1)	1298(1)	40(1)
O(3)	4964(2)	6989(1)	6564(1)	39(1)
O(4)	6473(2)	4563(1)	5878(1)	52(1)

Table 3. Bond lengths [Å] and angles [°] for GCA

C(1)-O(1)	1.2239(12)
C(1)-O(2)	1.2786(11)
C(1)-C(2)	1.5135(12)
C(2)-N(1)	1.4698(12)
C(2)-H(2A)	0.97
C(2)-H(2B)	0.97
C(3)-O(3)	1.2271(14)
C(3)-O(4)	1.2801(14)
C(3)-C(4)	1.5189(18)
C(4)-C(5)	1.4567(17)
C(4)-H(4A)	0.97
C(4)-H(4B)	0.97
C(5)-N(2)	1.1341(17)
N(1)-H(1A)	0.960(16)

N(1)-H(1C)	0.900(17)
N(1)-H(1B)	0.899(17)
O(2)-H(2)	1.2142(8)
O(4)-H(4)	1.2325(10)
O(1)-C(1)-O(2)	122.86(9)
O(1)-C(1)-C(2)	120.06(8)
O(2)-C(1)-C(2)	117.04(8)
N(1)-C(2)-C(1)	110.27(7)
N(1)-C(2)-H(2A)	109.6
C(1)-C(2)-H(2A)	109.6
N(1)-C(2)-H(2B)	109.6
C(1)-C(2)-H(2B)	109.6
H(2A)-C(2)-H(2B)	108.1
O(3)-C(3)-O(4)	125.43(11)
O(3)-C(3)-C(4)	121.32(10)
O(4)-C(3)-C(4)	113.23(10)
C(5)-C(4)-C(3)	113.24(10)
C(5)-C(4)-H(4A)	108.9
C(3)-C(4)-H(4A)	108.9
C(5)-C(4)-H(4B)	108.9
C(3)-C(4)-H(4B)	108.9
H(4A)-C(4)-H(4B)	107.7
N(2)-C(5)-C(4)	178.63(16)
C(2)-N(1)-H(1A)	110.5(9)
C(2)-N(1)-H(1C)	110.9(10)
H(1A)-N(1)-H(1C)	108.3(13)
C(2)-N(1)-H(1B)	110.7(10)
H(1A)-N(1)-H(1B)	108.9(14)
H(1C)-N(1)-H(1B)	107.5(14)
C(1)-O(2)-H(2)	116.09(7)
C(3)-O(4)-H(4)	113.71(9)

Symmetry transformations used to generate equivalent atoms:

Table 4. Hydrogen coordinates (x 10^4) and isotropic displacement parameters ($Å^2$x 10^3) for GCA

	x	y	z	U(eq)
H(2A)	5683	10520	1304	32
H(2B)	5753	8432	1864	32
H(4A)	8404	3879	8126	56
H(4B)	10003	5494	6949	56
H(1A)	4220(30)	8510(20)	4491(19)	48(4)
H(1C)	3800(30)	10490(20)	3790(18)	48(4)
H(1B)	2350(30)	9330(20)	3471(19)	53(4)
H(2)	10000	10000	0	92(9)
H(4)	5000	5000	5000	139(14)

The obtained diffraction peaks were indexed using 'TWO THETA' software package. Appearance of sharp and strong peaks confirms the good crystallinity of the grown sample. The indexed powder X-ray diffraction pattern is depicted in Fig. 6.

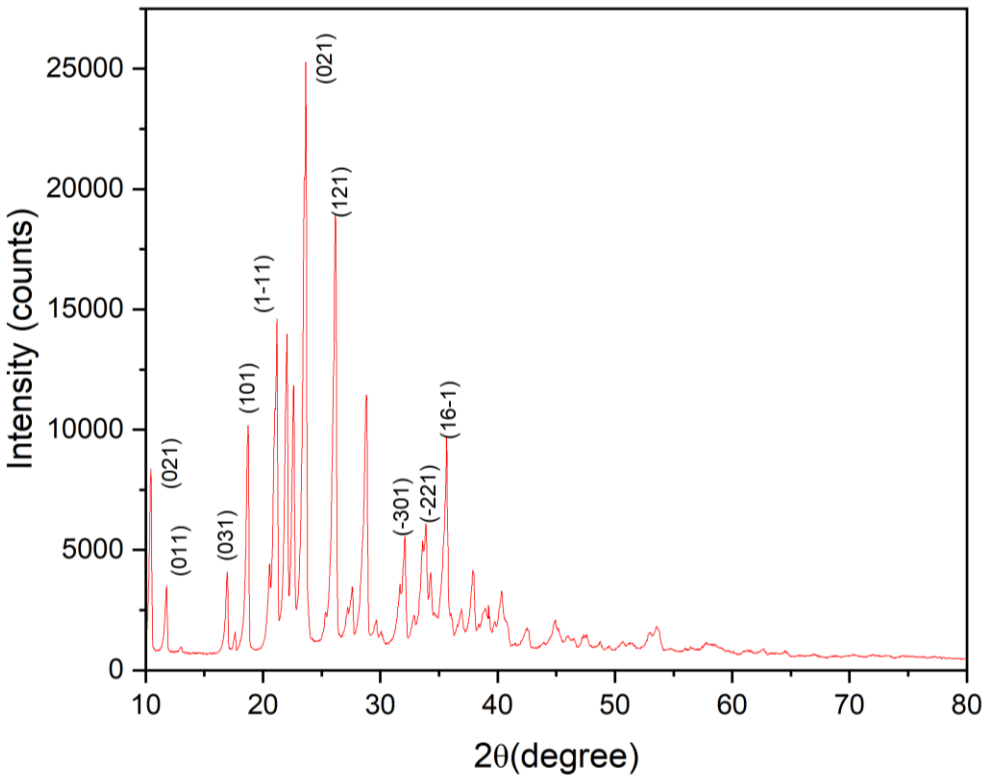

Fig 6.Indexed Powder x- ray diffraction of GCA crystal

Uv-Vis Studies

The crystal exhibits high transmittance over the visible range, as seen by the UV-Vis spectrum in Figure 9, making it a great material for optoelectronic applications. The signal cuts off at a lower wavelength of 324 nm is shown in Fig 7. When using diode and solid lasers, the low cutoff and excellent transparency are essential requirements for the frequency doubling process [16]. Transmission spectra were used to measure the optical band gap (Eg), and the optical absorption coefficient (h) close to the absorption edge is defined as $\alpha h\upsilon = A(h\upsilon - E_g)^2$

In this equation, A stands for a constant, Eg for the optical band gap, h for the Planck constant, and υ for the frequency of the input photons. The plot of $(\alpha h\upsilon)^{1/2}$ versus $h\upsilon$ (Fig. 8) was used to measure the GCA crystal's band gap and the value is found to be 3.62eV.

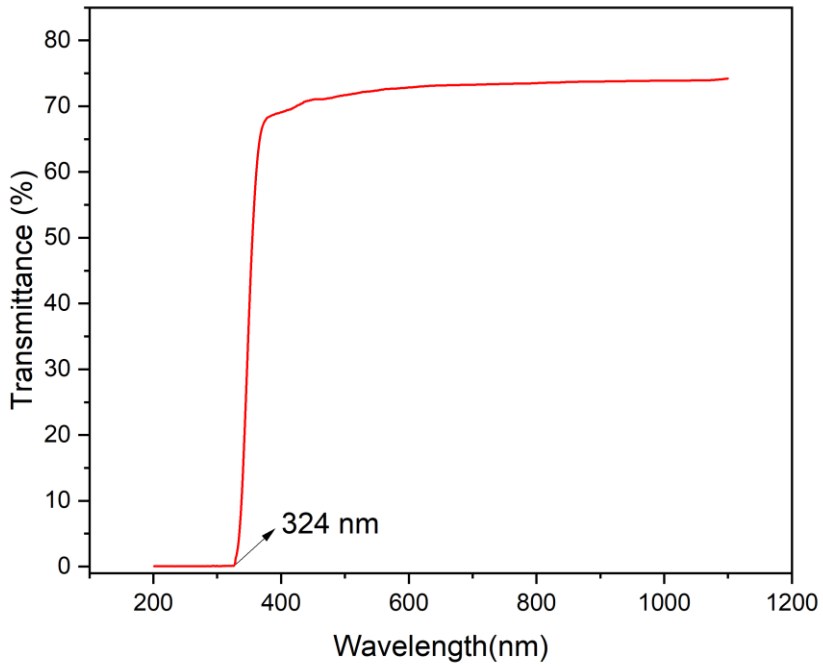

Fig 7. Transmittance spectrum of GCA Crystals

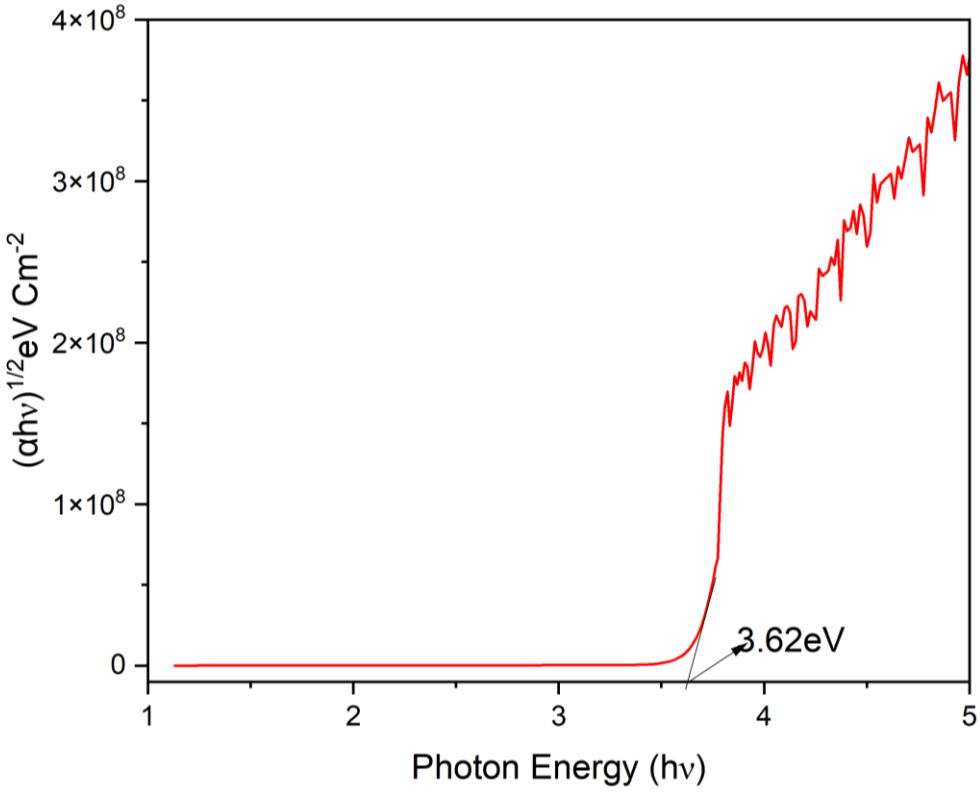

Fig 8. Band gap spectrum of GCA Crystals

Thermal Studies

Fig. 9 shows the thermogram of the GCA sample. The endothermic peak in the DTA curve was found around 110°C. However, there hasn't been a commensurate shift in the TG curve.

Therefore, a solid-state phase transition may be the cause of this endothermic peak. The DTA curve shows a prominent endothermic peak at 212 °C, which is the melting temperature of glycinium cyanoacetate crystal. The peak's sharpness indicates the sample's excellent purity and crystallinity. This is in line with observations of the material's melting behaviour made using the "MONARCH" melting device.

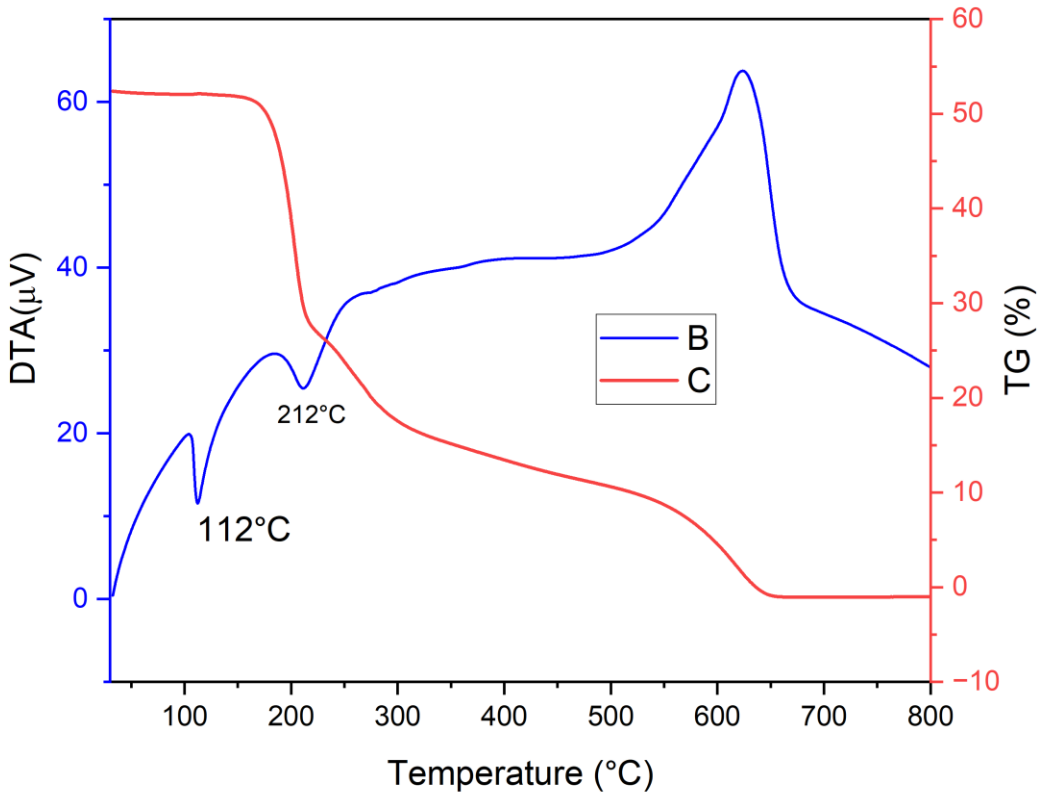

Fig 9.TG – DTA Curve of GCA

Microhardness

It should be noticed that the Vickers hardness number rises as the load rises. Observed in the produced GCA crystals is a reverse indentation size effect. Meyers law, which establishes a relationship between applied load and diagonal indentation length, was used to calculate the Meyers index number.

$$P = Kd^n$$

where n is the work hardening coefficient and K is the material constant.Fig 10 shows the plot of Log P vs Hardness number. Fig 11 displays the plot between log p and log d. Onitsch asserts that the value of n should be above 1.6 for softer material and between 1 and 1.6 for harder material [17-18]. The slope of log p Vs log d, which was used to determine the work hardening coefficient, is found to be more than 1.6. The GCA crystal thus belongs to the group of soft materials.

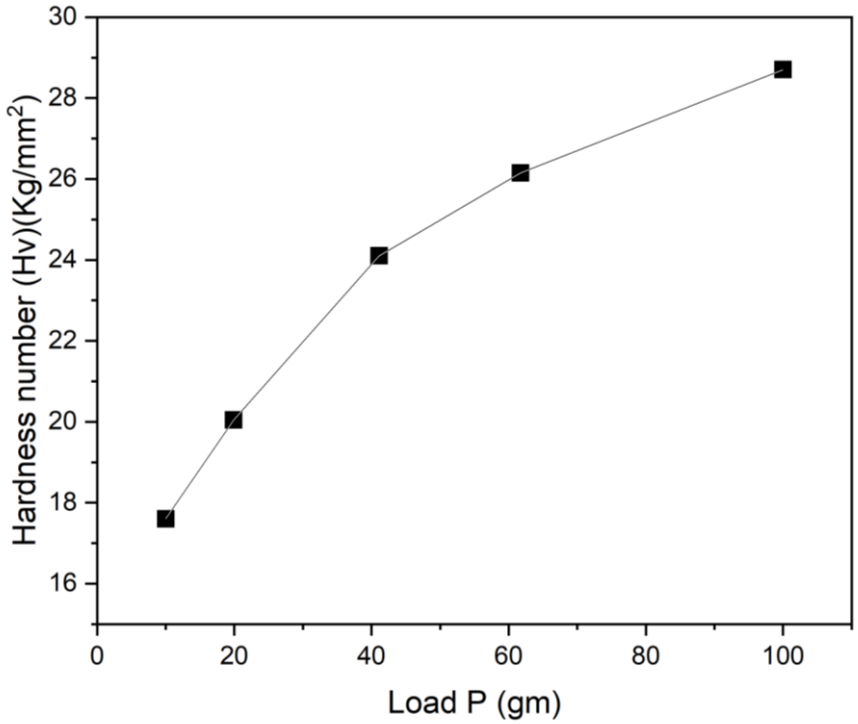

Fig 10. Log P vs Microhardness number

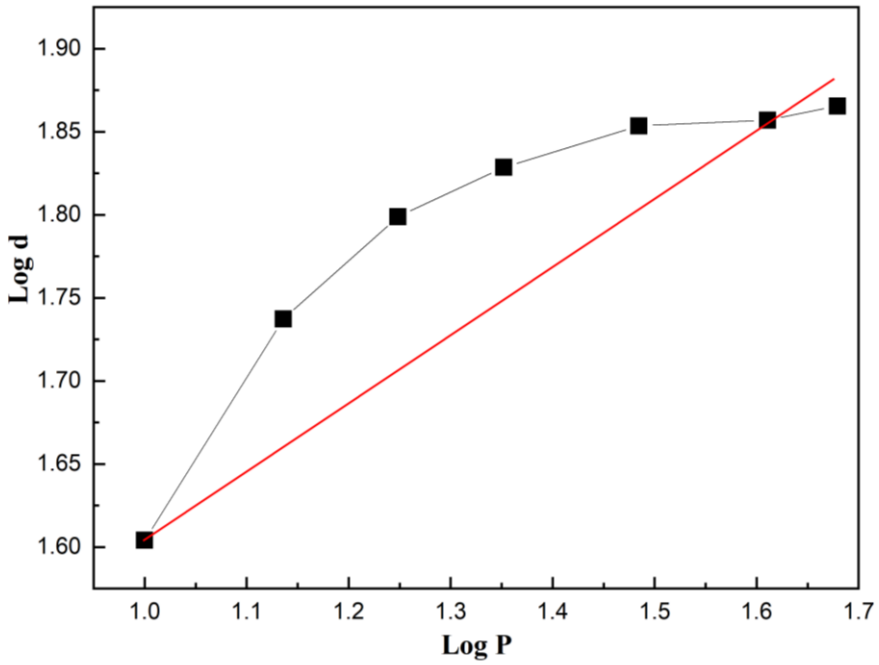

Fig 11. Log P vs log d of GCA Crystal

Laser Damage studies

The laser damage threshold property of the compound is influenced by factors like laser beam size, location, and longitudinal and transverse laser modes. Short pulse damage is controlled by optical breakdown and nonlinear recombination, whereas long pulse damage is controlled by heat conduction through the atomic lattice [19]. The energy density is calculated by using

$$P=E/\tau\pi r^2$$

Where E is the energy (mJ), τ- pulse width (ns) and r is the radius of the spot (mm). A crack is observed after passing 90 mJ energy in 30s. The average LDT of GCA single crystal is 1.3 GW/cm^2.

Antimicrobial Studies

By using the Well Diffusion method, the antibacterial and antifungal effects of crude extract extracts were assessed [20]. 20ml of molten medium were poured into sterilised petri plates to create MHA plates. A homogeneous 20–25 µl suspension of bacterial inoculums was swabbed after the media had solidified. The sterile paper discs were inserted in agar plates after being soaked in the necessary solvents. Following that, 10–50 µl of plant extract were added to the wells. The plates were then incubated for 24 hours at 37°C. Triplicates of the assay were performed, and control plates were kept as well. The zone of inhibition was measured in millimetres from the well's edge to the zone. A potato dextrose agar plate and mullerhintonagar plate were both covered with the tested cell solution. Wells were inserted using sterile forceps into the agar medium. Wells received a pouring of plant extract. Plates were then incubated for roughly 24 hours at 37°C while the control was likewise kept constant. From the clear zone, the zone of inhibition was measured in millimetres.

The agar diffusion method was used to perform antibacterial activity [21] By inoculating nutritive broth media with the stock culture of bacteria (K. Pnemoneae, Staphylococcus, Bacillus, and E. coli), the bacteria were obtained and grew at 37% for 18 hours. The above media's agar plates were made. Each plate was swabbed with germs from 18-hour-old cultures before being injected. Reduce the 5 wells. In ratios of 1%, 0.1%, 0.01%, and 0.001%, pour the extract. The diameter of the inhibitory zone on each plate was measured in cm after 24 hours of incubation at 37 °C.

Agar well diffusion method has been used to determine the antimicrobial activities and minimum inhibitory concentrations or plant extracts against Gram positive, Gram negative bacteria. The extracts exhibited antibacterial activities against tested microorganisms are shown in Table 4. Fig 12 shows the Inhibition zone of GCA again gram-positive and gram negative bacteria.

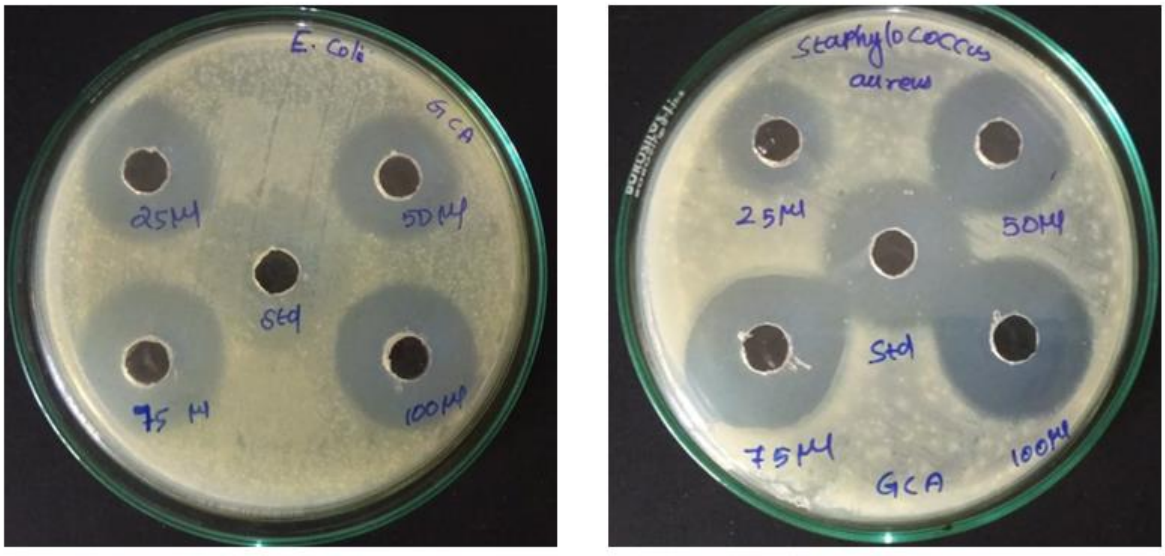

Fig 12 Inhibition zone of GCA again gram-positive and gram negative bacteria.

Table 5. Antibacterial activities of GCA Agar well diffusion method (inhibition zone in cm).

Concentration	***E.Coli***	***Staphylococcus aureus***
25 ul	0.9 cm	1.2 cm
50 ul	1.2 cm	1.5 cm
75 ul	1.7 cm	1.9 cm
100 ul	1.9 cm	2.0 cm
STD	1.8 cm	1.8 cm

Conclusion

In this study, the structure, growth, and characterisation of single crystals of GCA were described. The GCA single crystals were created using the slow evaporation solution growth method. It was determined from the single crystal XRD investigation that the crystal belongs to a Triclinic system with the space group P-1. It was discovered from UV-Vis spectra that there is no absorption throughout the entire visible range, which is a need for NLO applications. The TG-DTA technique was used to examine the compound's thermal stability and phase transition. Studies on antimicrobial agents revealed that GCA exhibits exceptional efficacy against gram-negative bacteria like *Staphylococcus aureus*. Because of the aforementioned findings, GCA crystals are supported as viable options for NLO and antibacterial applications.

Acknowledgment

The management of The M.D.T Hindu College, Pettai, Tirunelveli, is to be thanked for allowing the authors access to the department's research spaces including the DST-FIST sponsored instrumentation laboratory.

Declaration of competing interest

The authors declare that they have no known competing financial interests or personal relationships that could have appeared to influence the work reported in this paper.

References

1. A. Petrov, N. A. Belich, A. Y. Grishko, N. M. Stepanov, S. G. Dorofeev, E. G. Maksimov, A. V. Shevelkov, S. M. Zakeeruddin, M. Grätzel, A. B. Tarasov, E. A. Goodilin, *Materials Horizons*, 2017, 4, 625.
2. W. Zhang, X. Liu, L. Li, Z. Sun, S. Han, Z. Wu, J. Luo, *Chem. Mater.*, 2018, 30, 4081.
3. T. A. Shestimerova, N. A. Golubev, N. A. Yelavik, M. A. Bykov, A. V. Grigorieva, Z. Wei, E. V. Dikarev, A. V. Shevelkov, *Cryst. Growth Des.*, 2018, 18, 2572.
4. T. A. Shestimerova, N. A. Yelavik, A. V. Mironov, A. N. Kuznetsov, M. A. Bykov, A. V. Grigorieva, V. V. Utochnikova, L. S. Lepnev, A. V. Shevelkov, *Inorg. Chem.*, 2018, 57, 4077.
5. S. A. Adonin, M. N. Sokolov, V. P. Fedin, *Coord. Chem. Rev.*, 2018, 367, 16.
6. Sigdel Regmi, A. Apblett and D. Powell, *Acta Cryst.* (2020). E76, 1645-1648

7. N Sivakumar , N Kanagathara , G Bhagavannarayana , S Kalainathan , G Anbalagan Journal of Crystal Growth , volume 426 , p. 86 - 94 Posted: 2015
8. Bhawani Sigdel Regmi , Allen Apblettb , Douglas Powell, J.,Acta Cryst E , volume 76 , p. 1645 - 1648 Posted: 2020
9. B K Periyasamy , R S Jebas , N Gobalakrishnan , T Balasubramanian, Mater. Lett , volume 61 , p. 4246 - 4249 Posted: 2007
10. S. Muralidharan, P. Nagapandiselvi, A. Arun kumar, Solid State Communications, Volume 342, 2022, 114607,
11. N.F. Femi Frederic, D. Arul Dhas, I. Hubert Joe, B. Gunasekaran, S. Sindhusha, G. Vinitha,Journal of Molecular Structure,Volume 1274, Part 1,2023,134515,
12. S. Sivapriya, R. Subramaniyan Raja, A. Arun Kumar, J. Suryakanth, N. Arunadevi, E. Ranjith Kumar, K. Balasubramanian, ,Journal of Molecular Structure,Volume 1289, 2023,135822,
13. P Jayaprakash , M Peer , M Mohammed , Caroline Lydia, J. Mol. Struct , volume 1134 , p. 67 - 77 Posted: 2016
14. K Nivetha , S Kalainathan , M Yamada , Y Kondo , F Hamada Materials Chemistry and Physics , volume 188 , p. 131 - 142 Posted: 2017
15. Bruker, APEX2, SAINT and SADABS, Bruker AXS Inc., Madison,Wisconsin, USA, 2004.
16. G.M. Sheldrick, Short history of SHELX, ActaCrystallogr. Sect A. 64 (2008) 112–122.
17. *E.M. Onitsch, Mikroscopia 2 (1947) 131.*
18. M.Rajkumar, A.Chandramohan, Mater.Lett. 181, 354-357 (2016)
19. Arora S.K, Trivedi T.R and Patel V.A, Scripta Materials, 47, 643 (2002).
20. A.W. Bauer, M.D. and others, *American Journal of Clinical Pathology,* Volume 45, Issue 4_ts, April 1966, Pages 493–496,
21. P.J. van der Watt, *et al.* Mol. Canc. Therapeut., 15 (4) (2016), pp. 560-573